"Think how hard physics would be if particles could think."

— Murray Gell-Mann

CHAPTER 3

PROTON STRUCTURE FUNCTION AND GLUON DENSITY FROM BK EQUATION

In this chapter, we investigate the proton structure function $F_2^p(x, Q^2)$ at small-x using the analytical solution of the BK equation. In the color dipole description of DIS, the structure function $F_2^p(x, Q^2)$ is determined using the analytical expression for the scattering amplitude $N(k, Y)$ from the BK solution. In addition, we extract the integrated gluon density $xg(x, Q^2)$ using the BK solution and compare our theoretical estimate with the LHAPDF global data fits, NNPDF3.1sx and CT18. This chapter describes the behavior of $F_2^p(x, Q^2)$ in the kinematic area of $10^{-5} \leq x \leq 10^{-2}$ and $2.5 \leq Q^2 \leq 60$ GeV^2. Our predicted results for $F_2^p(x, Q^2)$ within the specific kinematic region are compared with the recent high precision data for $F_2^p(x, Q^2)$ from HERA (H1 collaboration) and the LHAPDF global parametrization group NNPDF3.1sx. This chapter is based on the article, which is ***"Investigation of proton structure function F_2^p at HERA in light of an analytical solution to Balitsky-Kovchegov equation", Communications in Theoretical Physics 76(3) (2024): 035202.***

3.1 Introduction

Comprehending the nucleon's substructure within matter is a fundamental study focus in high-energy particle physics. Understanding the structure of the nucleon is essential for grasping the fundamental composition of matter. The establishment of high-energy accelerator facilities has enabled us to comprehend the nucleon's substructure within the context of quantum chromodynamics (QCD). The comprehension of the nucleon's substructure has predominantly depended on its structure functions. Deep inelastic scattering (DIS) studies involving leptons and hadrons have provided substantial data regarding the distribution of partons within hadrons, specifically concerning quark and gluon distributions. The DIS cross section is associated with the structure functions of the nucleon in relation to parton distributions. The measurements of the proton's structure functions $F_2^p(x, Q^2)$ and $F_L^p(x, Q^2)$ at HERA have begun a new era of parton density measurement within the nucleon [1–4]. These structure functions can be correlated with the momentum distributions of partons within the nucleon and thus the parton distribution functions (PDFs). At high energies, or equivalently at small-x (Bjorken x) values, the gluon density dominates among partons, and hence the dominant contribution in $F_2^p(x, Q^2)$ and $F_L^p(x, Q^2)$ observations comes exclusively from gluons. Therefore, measurements of these structure functions at small-x are essential for calculating gluon distribution functions and visualizing the overall hadronic wave function in high-density QCD.

The DGLAP (Dokshitzer-Gribov-Lipatov-Altarelli-Parisi) evolution equation, a renowned and well-established framework, serves as a fundamental tool for the theoretical analysis of DIS structure functions. This equation has been effectively utilized to analyze the available HERA data in the moderate kinematic range of Bjorken's x ($x \geq 0.01$). At small-x, HERA data indicates a considerable increase in gluon behavior in that region. The pronounced behavior of gluons at small-x is

accurately characterized by the renowned BFKL (Balitsky-Fadin-Kuraev-Lipatov) evolution equation [10, 11]. Nonetheless, the rapid growth of gluons at small-x cannot persist indefinitely; otherwise, the physical cross-sections would contravene unitarity and the Froissart-Martin bound [12]. Consequently, both the DGLAP and BFKL evolution equations inadequately address the implicit physics in high-density QCD. To preserve the unitarity of the theory, the exponential growth of gluons must be mitigated by specific procedures. The phenomena of gluon recombination and saturation have resolved the issues encountered by the linear evolution equations [13–17]. The nonlinear phenomena of gluon recombination and saturation result in nonlinear components inside the DGLAP and BFKL equations. The Balitsky-Kovchegov (BK) equation, a nonlinear extension of the BFKL equation, along with the mean-field approximation of the Jalilian-Marian-Iancu-McLerran-Weigert-Leonidov-Kovner (JIMWLK) equation, elucidates the dynamics of gluon density in the small-x regime.

The collaborations at HERA provided high-precision data for the measurement of the proton structure function F_2^p throughout several kinematic regions of x and Q^2 [26, 27]. Recent studies on the measurement of proton structure functions utilizing diverse evolution equations and methodologies are detailed in Refs. [28–32], with results demonstrating strong correlation to experimental data. Reference [33] presents the inaugural examination of the reproduction of observations of the DIS proton structure function at high energy utilizing the color dipole framework in momentum space. Employing the understanding of asymptotic solutions of the BK equation, the authors of Ref. [33] quantified the charm structure function F_2^c as a function of x across several values of Q^2 and favorably contrasted their findings with those of the HERA experiment. At small-x, HERA has demonstrated that the contributions to parton distribution functions (PDFs) originate only from gluons. Consequently, ascertaining gluon density is crucial for comprehending the complete

hadronic wave function at small-x. This chapter focuses on extracting the gluon density $xg(x, Q^2)$ and examining the proton structure function F_2^p at small-x by integrating experimental data with QCD evolution theory through the analytical solution of the BK equation. We calculate the gluon density $xg(x, Q^2)$ and the proton structure function F_2^p over several kinematic areas of HERA and examine their characteristics at small-x.

The chapter's outline is as follows: In Section 3.2, we connect the dipole-proton cross-section to the forward scattering amplitude inside the color dipole framework of deep inelastic scattering in quantum chromodynamics. Subsequently, with the analytical solution of the BK equation, we examine how the structure function F_2^p of the proton can be derived from the color dipole framework. In Section 3.3, we provide the x evolution of the integrated gluon density $xg(x, Q^2)$ for two values of Q^2, specifically 35 GeV^2 and 100 GeV^2, utilizing the BK evolution theory. Our findings are compared with the PDF data fits NNPDF3.1sx [34] and CT18 [35]. Both analyses incorporate data from LHC and HERA. The numerical results for the proton structural function F_2^p, derived from the analytical solution of the BK equation, are presented alongside data from the H1 Collaboration and the NNPDF3.1sx parameterization group. Section 3.4 succeeds the chapter summary discussion.

3.2 Proton's Structure function in the Color Dipole Description

As per the color dipole model [36–38], DIS transpires when a color dipole, predominantly a quark-antiquark ($q\bar{q}$) pair, engages with the proton. The transverse dimensions of the pair are represented by $\mathbf{r}$, with each quark possessing a fraction z of the photon's light-cone momentum. The dipole lifetime in the proton rest

frame significantly exceeds the time necessary for interaction with the target proton. The elastic $\gamma^* p$ scattering transpires in three phases: initially, the arriving virtual photon fluctuates into a $q\bar{q}$ pair; subsequently, the $q\bar{q}$ pair undergoes elastic scattering with the proton; and ultimately, the $q\bar{q}$ pair recombines to produce a virtual photon. The elastic process $\gamma^* p \to \gamma^* p$ possesses an amplitude denoted as $\mathcal{A}^{\gamma^* p}(x, Q, \Delta)$, expressed as

$$\mathcal{A}^{\gamma^* p}(x, Q, \Delta) = \sum_f \sum_{h,\bar{h}} \int d^2\mathbf{r} \int_0^1 dz \Psi^*_{h\bar{h}}(r, z, Q) \mathcal{A}_{q\bar{q}}(x, r, \Delta) \Psi_{h\bar{h}}(r, z, Q). \quad (3.1)$$

Where $\mathcal{A}_{q\bar{q}}(x, r, \Delta)$ denotes the fundamental amplitude for the scattering of a dipole of size $\mathbf{r}$ on the proton, Δ signifies the transverse momentum lost by the outgoing proton, and x is the Bjorken variable. The amplitude of the entering virtual photon, $\Psi_{h\bar{h}}(r, z, Q)$, denotes the amplitude for the dipole with helicities h and $\bar{h}$, and flavor f.

The fundamental scattering amplitude $\mathcal{A}_{q\bar{q}}$ is defined so that the elastic differential cross-section for the $q\bar{q}$ pair scattering off the proton is

$$\frac{d\sigma_{q\bar{q}}}{dt} = \frac{1}{16\pi} |\mathcal{A}_{q\bar{q}}(x, r, \Delta)|^2, \quad (3.2)$$

where $t = -\Delta^2$. It can be related to the S-matrix element $S(x, r, b)$ for the scattering of a dipole of size $\mathbf{r}$ at impact parameter $\mathbf{b}$ as

$$\mathcal{A}_{q\bar{q}}(x, r, \Delta) = \int d^2\mathbf{b} e^{-i\mathbf{b}.\boldsymbol{\Delta}} \mathcal{A}_{q\bar{q}}(x, r, b) = i \int d^2\mathbf{b} e^{-i\mathbf{b}.\boldsymbol{\Delta}}\, 2[1 - S(x, r, b)]. \quad (3.3)$$

The dipole-proton cross-section, $\sigma_{q\bar{q}}(x, r)$, can be obtained from the elastic dipole-proton scattering amplitude $\mathcal{A}_{q\bar{q}}$ using the optical theorem as [33]

$$\sigma_{q\bar{q}}(x, r) = \text{Im}\mathcal{A}_{q\bar{q}}(x, r, \Delta = 0) = \int \frac{d^2\sigma_{q\bar{q}}}{d^2\mathbf{b}}(x, r, \mathbf{b}) d^2\mathbf{b} = 2\pi R_p^2 N(x, r), \quad (3.4)$$

where the proton radius is denoted by R_p^2; for the purpose of this work, its value will be taken from recent work on the proton radius [40], which is $R_p \approx 0.831\text{fm} \approx 4.22$ GeV^{-1}. The solution of the BK evolution equation yields the dipole-proton scattering amplitude $N(x, r)$, which provides information about the strong interaction of the quark-antiquark dipole.

The total cross-section for $\gamma^* p$ scattering is obtained using (3.1) and (3.4) as [41]

$$\sigma_{T,L}^{\gamma^* p} = \sum_f \int \mathrm{d}^2\mathbf{r} \int_0^1 \mathrm{d}z (\Psi^*\Psi)_{T,L}^f \sigma_{q\bar{q}}(x, r), \tag{3.5}$$

where $\Psi^*\Psi)_{T,L}^f$, the overlap of the photon wave functions defined as

$$\begin{aligned} (\Psi^*\Psi)_T^f &= \frac{1}{2} \sum_{h,\bar{h}} \Big[\Psi^*_{h\bar{h},\lambda=+1} \Psi_{h\bar{h},\lambda=+1} + \Psi^*_{h\bar{h},\lambda=-1} \Psi_{h\bar{h},\lambda=-1} \Big], \\ (\Psi^*\Psi)_L^f &= \sum_{h,\bar{h}} \Psi^*_{h\bar{h},\lambda=0} \Psi_{h\bar{h},\lambda=0}, \end{aligned} \tag{3.6}$$

where T, L represent the transverse and longitudinal polarization states of the virtual photon, respectively. λ denotes the photon helicity and f, the flavor of the quark-antiquark pair. After obtaining the $\gamma^* p$ cross-section, one can obtain directly the proton structure function F_2^p from the $\gamma^* p$ cross-section through the relation

$$F_2^p(x, Q^2) = \frac{Q^2}{4\pi^2 \alpha_{em}} \Big[\sigma_T^{\gamma^* p}(x, Q^2) + \sigma_L^{\gamma^* p}(x, Q^2) \Big]. \tag{3.7}$$

The photon wave functions can be represented using the Bessel functions K_0 and K_1. These wave functions rely on the quark mass m_f and quark electric charge $e_f = 2/3, -1/3$ through

$$|\Psi_L^f(r, z; Q^2)|^2 = e_f^2 \frac{\alpha_{em} N_c}{2\pi^2} 4Q^2 z^2 (1-z)^2 K_0^2(r\bar{Q}_f), \tag{3.8a}$$

$$|\Psi_T^f(r,z;Q^2)|^2 = e_f^2\frac{\alpha_{em}N_c}{2\pi^2}\Big([z^2+(1-z)^2]\bar{Q}_f^2K_1^2(r\bar{Q}_f)+m_f^2K_0^2(r\bar{Q}_f)\Big), \quad (3.8b)$$

where $\bar{Q}_f^2 = z(1-z)Q^2+m_f^2$, m_f is the mass of the quark of flavor f, α_{em} is the electromagnetic fine-structure constant, and N_c is the number of colors.

Let's now express the γ^*p cross-section in $N(k,Y)$. For this, let us transform $N(r,Y)$ to $N(k,Y)$ using the following simple Fourier transform.

$$\begin{aligned} N(k,Y) &= \frac{1}{2\pi}\int\frac{d^2r}{r^2}e^{ik.r}N(r,Y) \\ &= \int_0^\infty\frac{dr}{r}J_0(kr)N(r,Y). \end{aligned} \quad (3.9)$$

The proton structure function F_2^p in momentum space related to $N(k,Y)$ can be expressed as follows using the discussion from above and some algebraic calculations

$$F_2^p(x,Q^2) = \frac{Q^2R_p^2N_c}{4\pi^2}\int_0^\infty\frac{dk}{k}\int_0^1 dz|\Psi(k^2,z;Q^2)|^2N(k,Y), \quad (3.10)$$

where the photon wave function Ψ is now expressed in the momentum space, which is given by [33]

$$\begin{aligned} |\Psi(k^2,z;Q^2)|^2 = \sum_f\left(\frac{4\bar{Q}_f^2}{k^2+4\bar{Q}_f^2}\right)e_f^2\Bigg\{&[z^2+(1-z)^2] \\ &\left[\frac{4(k^2+\bar{Q}_f^2)}{k^2\sqrt{k^2+4\bar{Q}_f^2}}\,\text{arcsinh}\Big(\frac{k^2}{2\bar{Q}_f}\Big)+\frac{k^2-2\bar{Q}_f^2}{2\bar{Q}_f^2}\right] \\ &+\frac{4Q^2z^2(1-z)^2+m_f^2}{\bar{Q}_f^2}\left[\frac{k^2+\bar{Q}_f^2}{\bar{Q}_f^2}\right. \\ &\left.-\frac{4\bar{Q}_f^4+2\bar{Q}_f^2k^2+k^4}{\bar{Q}_f^2\sqrt{k^2(k^2+4\bar{Q}_f^2)}}\,\text{arcsinh}\Big(\frac{k}{2\bar{Q}_f}\Big)\right]\Bigg\}. \end{aligned} \quad (3.11)$$

The scattering amplitude $N(k,Y)$ comes from the solution of the BK equation,

presented in the previous chapter (see equation (2.26)), given by

$$N(k,Y) = \frac{e^{Y-k^2/Q_{s0}^2}}{1 - e^{-k^2/Q_{s0}^2} + e^{Y-k^2/Q_{s0}^2}}, \tag{3.12}$$

where Q_{s0}^2 is the squared value of the initial saturation momentum of gluons that can be fitted from the existing HERA data, and its value is 0.24 GeV^2.

3.3 Results and Discussion

We employed the equation (3.10) alongside the analytical solution of the BK equation (3.12) to examine the proton structure function F_2^p. We numerically solved the equation (3.10) for several values of x and Q^2. In equation (3.10), $\Psi(k^2, z; Q^2)$ denotes the probability of a virtual photon producing a quark-antiquark pair, where the quark possesses a momentum fraction z and the antiquark $(1-z)$ of the virtual photon in momentum space, as articulated in equation (3.11). We shall examine the behavior of the formula (3.11) with respect to transverse momentum k for different values of Q^2, assuming $m_f \to 0$ and $z = 1/2$ (where $0 < z < 1$). The probability distribution graph of the virtual photon emitting a quark-antiquark pair with $z = 1/2$ as a function of transverse momentum k is illustrated in Figure 3.1. The probability to emit a quark-antiquark pair increases as k increases until a certain point (peak point), after which it decreases as k increases. The peak point for every Q^2 value is the same, but the transverse momentum k corresponding to every peak is different for Q^2.

The solution (3.12) gives the propagation of the quark-antiquark dipole in the color dipole description of QCD, which in turn gives the content of the proton, i.e. the unintegrated gluon density. To calculate conventional gluon density $xg(x, Q^2)$, we integrated the BK solution (3.12) over transverse momentum with the relation,

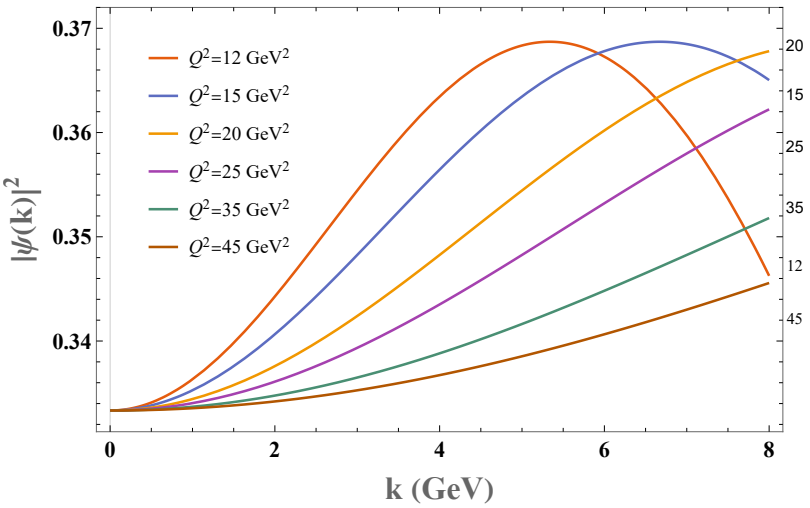

Figure 3.1: The probability distribution of the virtual photon to emit a quark-antiquark pair as a function of k with $m_f \to 0$ and $z = 1/2$ for values of Q^2.

given by

$$xg(x, Q^2) = \int_0^{Q^2} \frac{dk}{k} N(k, Y). \tag{3.13}$$

We estimated the gluon density for two Q^2 values, viz., $Q^2 = 35$ GeV^2 and $Q^2 = 100$ GeV^2. We presented a comparison between our estimated integrated gluon density and the gluon density predicted by the LHAPDF global parameterization groups CT18 [35] and NNPDF3.1sx [34]. Both the HERA and the most current LHC data with highly precise PDF sensitivity measurements are included in the LHAPDF datasets. The results are shown in Figure 3.2. To check the strength of the gluon

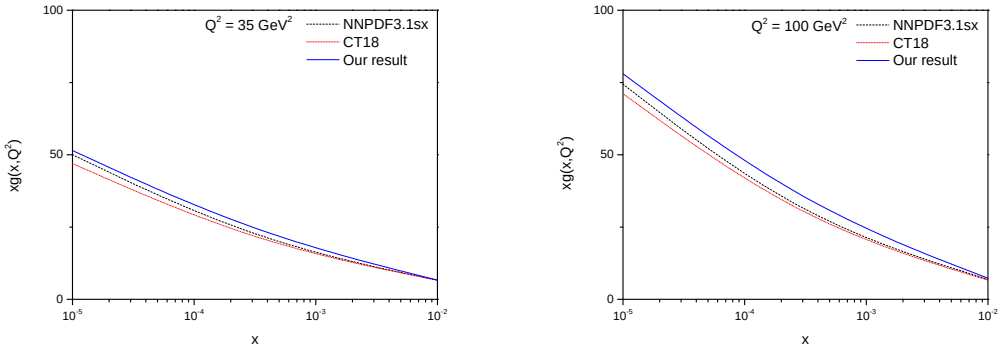

Figure 3.2: x-evolution of gluon density $xg(x, Q^2)$ extracted from the solution of the BK equation compared with the global data fits NNPDF3.1sx [34] and CT18 [35].

emission process inside the proton, we define a quantity given by

$$\lambda_{eff} = \frac{d \ln \left(x g(x, Q^2) \right)}{d \ln \left(\frac{1}{x} \right)}. \tag{3.14}$$

This is the logarithmic rate of rise of the gluon distribution function or the gluon density with different x values. We plotted this quantity as a function of x at different dipole sizes r in order to check the strength of the gluon emission process. The result is shown in Figure 3.3.

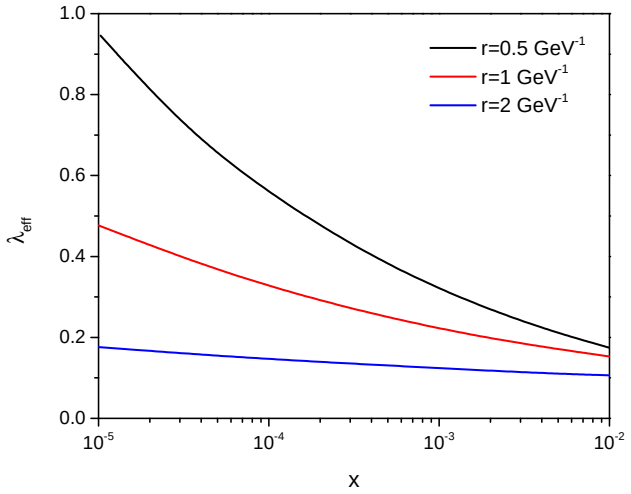

Figure 3.3: The logarithmic rate of rise of the gluon distribution function as a function of x at different dipole sizes r.

For the proton structure function F_2^p, we put the expression given in equation (3.11) (with $m_f \to 0$ and $z = 1/2$) together with the solution of the BK equation given in equation (3.12) into equation (3.10). We set $N_c = 3$ and $R_p \approx 0.831$ fm ≈ 4.22 GeV^{-1} in the expression equation (3.10) and solve the expression numerically for various Q^2. We analyzed the equation (3.10) and compared our results with the HERA measurements of the proton structure function from H1 Collaboration [27] with constraints to the kinematic region: $10^{-5} \leq x \leq 10^{-2}$ and $2.5 \leq Q^2 \leq 60$ GeV^2. We also compared our results with the LHAPDF global parameterization

group NNPDF3.1sx [34]. The reason for choosing the particular kinematic region $x \leq 10^{-2}$ is to describe the small-x behavior of high-energy amplitude as the BK equation is only applicable at small-x. For the Q^2 range, which is too high, we would need corrections from the DGLAP equation, which we cannot skip at high Q^2. The results are shown below in Figure 3.4.

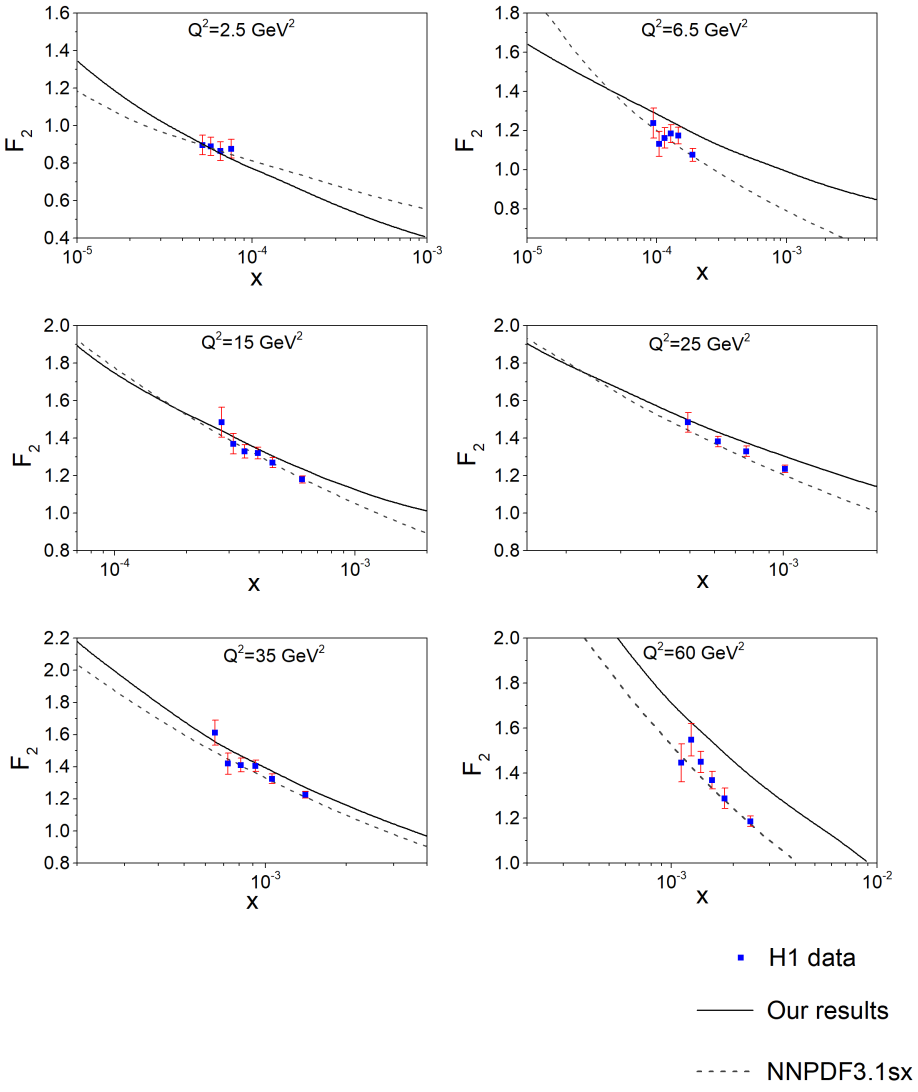

Figure 3.4: The results of the proton structure function F_2^p as a function of x at various Q^2 obtained in this work are compared with the data from H1 Collaboration [27] and global data fit NNPDF3.1sx [34].

3.4 Summary

In this chapter, we investigated the proton structure function F_2^p in light of an analytical solution of the BK equation. Proton structure functions have been investigated by different collaborations at experimental facilities such as HERA and the LHC. On the phenomenological side, the proton structure functions have been investigated by employing different QCD evolution equations and tested well at existing experimental facilities. To investigate the proton structure functions at small-x, the BK equation is most suitable for testing the experimental data on observables. This chapter initiates our examination of how to derive the proton structure function F_2^p from the color dipole framework of DIS in quantum chromodynamics (QCD). In the color dipole framework, the proton structure function F_2^p is derived directly from the virtual photon-proton cross-section, which can be articulated in terms of the dipole-proton scattering amplitude $N(k, Y)$. The dipole-proton scattering amplitude $N(k, Y)$ is obtained from the solution of the BK equation. Utilizing the solution of the BK equation, we derived the x evolution of the integrated gluon density $xg(x, Q^2)$ and compared our findings with the LHAPDF global data fits NNPDF3.1sx and CT18. Both NNPDF3.1sx and CT18 have used HERA and LHC data into their studies. Furthermore, we assessed the intensity of gluon emission processes by graphing the logarithmic rate of increase of gluon distribution as a function of x for various dipole sizes r. Figure 3.3 indicates that as one transitions from the large-x to the small-x region, the intensity of the gluon density escalates for diminutive dipole sizes. Nonetheless, as we augment the dipole size, the strength diminishes in comparison to lower dipole sizes. This simply indicates that gluons generated from greater dipole sizes become saturated. It demonstrates that gluons at small-x not only emit additional gluons but also undergo saturation, hence corroborating the phenomena of gluon saturation at small-x. It is an essential outcome that we

achieved by our analytical solution of the BK equation. Ultimately, we calculated the proton structural function F_2^p and contrasted it with the measurement of F_2^p at HERA from the H1 Collaboration and the LHAPDF global parameterization group NNPDF3.1sx. Our anticipated outcomes align well with the experimental results within the defined kinematic domain. Beyond that, we have to consider corrections to the DGLAP equation. We have also shown in this work how the virtual photon wave function Ψ would behave against transverse momentum k with $m_q \to 0$ and $z = 1/2$ at various Q^2. We found that the probability of the virtual photon emitting a quark-antiquark pair increases as k increases to a certain peak value, after which it starts to fall as k increases. We have seen that the maximum probability is the same for different Q^2 values, irrespective of the value of k at the maximum peak for different Q^2 values.

In this chapter, we have seen the ability of the analytical solution of the BK equation to describe nonlinear physics at small-x. We have successfully applied our analytical solution to calculate the gluon density $xg(x, Q^2)$ and the proton's structure function F_2^p at small-x within the kinematic region we have constrained. Moreover, our results are testable at future experimental facilities such as the LHeC (Large Hadron electron Collider) [42, 43], the EIC (Electron Ion Collider) [44], and the FCC-eh (Future Circular Collider electron-hadron) [45]. In these future experimental facilities, the measurement of the proton structure function will be performed at much lower values of x with increased precision. Nevertheless, we could investigate the proton structure function F_2^p using an analytical solution of the BK equation within the constrained region. We conclude that the analytical solution of the BK equation can serve as a convenient tool for further studies at small-x and high-density QCD. We hope that the BK equation, together with future experimental facilities, will help us to understand and to explore phenomena inside hadrons at small-x in the near future.

Bibliography

[1] M Derrick, D Krakauer, S Magill, B Musgrave, J Repond, S Repond, R Stanek, RL Talaga, J Thron, F Arzarello, et al. Measurement of the proton structure function f2 in ep scattering at hera. *Physics Letters B*, 316(2-3):412–426, 1993.

[2] I Abt, T Ahmed, V Andreev, B Andrieu, R-D Appuhn, M Arpagaus, A Babaev, H Bärwolff, J Ban, P Baranov, et al. Measurement of the proton structure function f2 (x, q2) in the low-x region at hera. *Nuclear Physics B*, 407(3):515–535, 1993.

[3] T Ahmed, S Aid, A Akhundov, V Andreev, B Andrieu, R-D Appuhn, M Arpagaus, A Babaev, J Baehr, J Ban, et al. A measurement of the proton structure function f2 (x, q2). *Nuclear Physics B*, 439(3):471–502, 1995.

[4] Catherine Adloff, S Aid, M Anderson, V Andreev, B Andrieu, C Arndt, A Babaev, J Bähr, J Ban, Y Ban, et al. Determination of the longitudinal proton structure function fl (x, q2) at low x. *Physics Letters B*, 393(3-4):452–464, 1997.

[5] VN Gribov and LN Lipatov. Deep inelastic electron scattering in perturbation theory. *Physics Letters B*, 37(1):78–80, 1971.

[6] V Gribov and L Lipatov. e+ e-pair annihilation and deep inelastic ep scattering in perturbation theory. *Soviet Journal of Nuclear Physics*, 15:675–675, 1972.

[7] LN Lipatov. The parton model and perturbation theory. *Yad. Fiz.*, 20:94–102, 1975.

[8] Guido Altarelli and Giorgio Parisi. Asymptotic freedom in parton language. *Nuclear Physics B*, 126(2):298–318, 1977.

[9] Yuri L Dokshitzer. Calculation of the structure functions for deep inelastic scattering and e+ e-annihilation by perturbation theory in quantum chromodynamics. *Zh. Eksp. Teor. Fiz*, 73:1216, 1977.

[10] EA Kuraev, LN Lipatov, and VS Fadin. The pomeranchuk singularity in nonabelian gauge theories. *Sov. Phys. JETP*, 45:199, 1977.

[11] Yu Yu Balitsky and LN Lipatov. The pomeranchuk singularity in quantum chromodynamics. *Yad. Fiz.*, 28:1597–1611, 1978.

[12] Marcel Froissart. Asymptotic behavior and subtractions in the mandelstam representation. *Physical Review*, 123(3):1053, 1961.

[13] LV Gribov, EM Levin, and MG Ryskin. Singlet structure function at small x: Unitarization of gluon ladders. *Nuclear Physics B*, 188(3):555–576, 1981.

[14] Leonid Vladimirovič Gribov, Eugene M Levin, and Michail G Ryskin. Semihard processes in qcd. *Physics Reports*, 100(1-2):1–150, 1983.

[15] Alfred H Mueller and Jianwei Qiu. Gluon recombination and shadowing at small values of x. *Nuclear Physics B*, 268(2):427–452, 1986.

[16] Alfred H Mueller. Small-x behavior and parton saturation: A qcd model. *Nuclear Physics B*, 335(1):115–137, 1990.

[17] Wei Zhu and Jianhong Ruan. A new modified altarelli-parisi evolution equation with parton recombination in proton. *Nuclear Physics B*, 559(1-2):378–392, 1999.

[18] Ian Balitsky. Operator expansion for diffractive high-energy scattering. *arXiv preprint hep-ph/9706411*, 1997.

[19] Yuri V Kovchegov. Small-x f 2 structure function of a nucleus including multiple pomeron exchanges. *Physical Review D*, 60(3):034008, 1999.

[20] Yuri V Kovchegov. Unitarization of the bfkl pomeron on a nucleus. *Physical Review D*, 61(7):074018, 2000.

[21] Ian Balitsky. Effective field theory for the small-x evolution. *Physics Letters B*, 518(3-4):235–242, 2001.

[22] Ian Balitsky. Operator expansion for high-energy scattering. *Nuclear Physics B*, 463(1):99–157, 1996.

[23] Jamal Jalilian-Marian, Alex Kovner, Andrei Leonidov, and Heribert Weigert. The bfkl equation from the wilson renormalization group. *Nuclear Physics B*, 504(1-2):415–431, 1997.

[24] Edmond Iancu, Andrei Leonidov, and Larry McLerran. Nonlinear gluon evolution in the color glass condensate: I. *Nuclear Physics A*, 692(3-4):583–645, 2001.

[25] Heribert Weigert. Unitarity at small bjorken x. *Nuclear Physics A*, 703(3-4):823–860, 2002.

[26] Francise D Aaron, H Abramowicz, I Abt, L Adamczyk, M Adamus, Al-daya Martin, C Alexa, V Andreev, S Antonelli, P Antonioli, et al. Combined measurement and qcd analysis of the inclusive e±p scattering cross sections at hera. *Journal of High Energy Physics*, 2010(1):1–63, 2010.

[27] H1 Collaboration, V Andreev, A Baghdasaryan, S Baghdasaryan, K Begzsuren, A Belousov, P Belov, V Boudry, G Bradt, M Brinkmann, et al. Measurement of inclusive ep ep cross sections at high qˆ 2 q 2 at s= 225 s= 225 and 252 gev

and of the longitudinal proton structure function f _ l fl at hera. *The European Physical Journal C*, 74:1–26, 2014.

[28] Pragyan Phukan, Madhurjya Lalung, and Jayanta Kumar Sarma. Studies on gluon evolution and geometrical scaling in kinematic constrained unitarized bfkl equation: application to high-precision hera dis data. *The European Physical Journal C*, 79:1–25, 2019.

[29] Pragyan Phukan, Madhurjya Lalung, and Jayanta Kumar Sarma. Small x phenomenology on gluon evolution through the bfkl equation in light of a constraint in multi-regge kinematics. *Communications in Theoretical Physics*, 72(2):025201, 2020.

[30] Madhurjya Lalung, Pragyan Phukan, and Jayanta K Sarma. On analytical solutions of proton's structure functions in the framework of glr–mq-zrs equation. *Results in Physics*, 28:104551, 2021.

[31] GR Boroun and B Rezaei. An evaluation of the proton structure functions f2 and fl at small x. *Physics Letters B*, 816:136274, 2021.

[32] GR Boroun. Nonlinear corrections to the longitudinal structure function fl from the parametrization of f 2: Laplace transform approach. *The European Physical Journal Plus*, 137(3):371, 2022.

[33] JT de Santana Amaral, Maria Beatriz Gay Ducati, MA Betemps, and Gregory Soyez. γ^* p cross section from the dipole model in momentum space. *Physical Review D—Particles, Fields, Gravitation, and Cosmology*, 76(9):094018, 2007.

[34] Richard D Ball, Valerio Bertone, Stefano Carrazza, Luigi Del Debbio, Stefano Forte, Patrick Groth-Merrild, Alberto Guffanti, Nathan P Hartland, Zahari Kassabov, José I Latorre, et al. Parton distributions from high-precision collider data: Nnpdf collaboration. *The European Physical Journal C*, 77:1–75, 2017.

[35] Tie-Jiun Hou, Jun Gao, TJ Hobbs, Keping Xie, Sayipjamal Dulat, Marco Guzzi, Joey Huston, Pavel Nadolsky, Jon Pumplin, Carl Schmidt, et al. New cteq global analysis of quantum chromodynamics with high-precision data from the lhc. *Physical Review D*, 103(1):014013, 2021.

[36] Nikolai N Nikolaev and BG Zakharov. Colour transparency and scaling properties of nuclear shadowing in deep inelastic scattering. *Zeitschrift für Physik C Particles and Fields*, 49(4):607–618, 1991.

[37] Alfred H Mueller. Soft gluons in the infinite-momentum wave function and the bfkl pomeron. *Nuclear Physics B*, 415(2):373–385, 1994.

[38] Alfred H Mueller and Bimal Patel. Single and double bfkl pomeron exchange and a dipole picture of high energy hard processes. *Nuclear Physics B*, 425(3):471–488, 1994.

[39] H Kowalski, L Motyka, and G Watt. Exclusive diffractive processes at hera within the dipole picture. *Physical Review D—Particles, Fields, Gravitation, and Cosmology*, 74(7):074016, 2006.

[40] W Xiong, A Gasparian, H Gao, D Dutta, M Khandaker, N Liyanage, E Pasyuk, C Peng, X Bai, L Ye, et al. A small proton charge radius from an electron–proton scattering experiment. *Nature*, 575(7781):147–150, 2019.

[41] AM Staśto, K Golec-Biernat, and J Kwieciński. Geometric scaling for the total γ^* p cross section in the low x region. *Physical Review Letters*, 86(4):596, 2001.

[42] JL Abelleira Fernandez, C Adolphsen, Ahmet Nuri Akay, H Aksakal, JL Albacete, S Alekhin, P Allport, V Andreev, RB Appleby, E Arikan, et al. A large hadron electron collider at cern report on the physics and design concepts for

machine and detector. *Journal of Physics G: Nuclear and Particle Physics*, 39(7):075001, 2012.

[43] P Agostini, H Aksakal, S Alekhin, PP Allport, N Andari, KDJ Andre, D Angal-Kalinin, S Antusch, L Aperio Bella, L Apolinario, et al. The large hadron–electron collider at the hl-lhc. *Journal of Physics G: Nuclear and Particle Physics*, 48(11):110501, 2021.

[44] A Accardi, JL Albacete, M Anselmino, N Armesto, EC Aschenauer, Alessandro Bacchetta, D Boer, WK Brooks, T Burton, N B Chang, et al. Electron-ion collider: The next qcd frontier: Understanding the glue that binds us all. *The European Physical Journal A*, 52:1–100, 2016.

[45] Asmaa Abada, Marcello Abbrescia, Shehu S AbdusSalam, I Abdyukhanov, J Abelleira Fernandez, A Abramov, Mohamed Aburaia, AO Acar, PR Adzic, Prateek Agrawal, et al. Fcc physics opportunities. *The European Physical Journal C*, 79(6):1–161, 2019.